

Supplementary information

Hollow Cubic Ternary PdCuB Nanocages Electrocatalyst with Greatly Enhanced Catalytic Performance for Formic Acid Oxidation

Fu-Kai Yang,^a Yue Fang,^a BingTao Gong,^a Wei-Li Qu,^{a,b,} Chao Deng,^a Zhen-Bo Wang^c*

Experimental Section

Materials

Palladium (II) chloride (PdCl_2 , 99%) was purchased from J&K Scientific, cupric chloride anhydrous ($\text{CuCl}_2 \cdot 2\text{H}_2\text{O}$, 99.99%), acetic acid ($\text{C}_2\text{H}_4\text{O}_2$, $\geq 99.8\%$), N, N-dimethylformamide (DMF) was bought from Macklin, polyvinylpyrrolidone (PVP, MW: 8000), ascorbic acid ($\text{C}_6\text{H}_8\text{O}_6$), formic acid (HCOOH) were purchased from Sinopharm Chemical Reagent Co. Ltd, NaBH_4 purchased from Tianjin Aoran Fine Chemical Research Institute.

Preparation of PdCuB nanocages

Syntheses of Cu_2O nanocubes

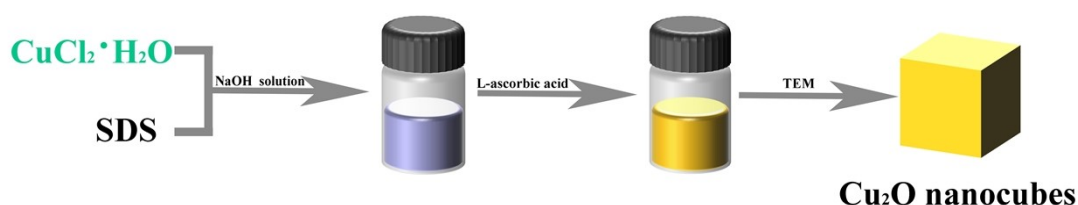


Fig. S1 Schematic diagram of Cu_2O preparation process

Typically, Cu_2O nanocubes are synthesized in a pot of wet process at room temperature (Fig. S1). Firstly, 144.2 mg sodium dodecyl sulfate was dissolved with 5 mL ultrapure water in a 20 mL glass bottle, then 38.6 mg $\text{CuCl}_2 \cdot 2\text{H}_2\text{O}$ was added and ultrasonic oscillation was carried out until all solids were dissolved. Then 0.9 mL NaOH aqueous solution (0.5M) was injected into the solution at one time through a pipette under intense agitation, and the reaction was maintained for 10 minutes to obtain the ultramin flocculant precursor. After that, 2.0 mL ascorbic acid aqueous solution (0.1M) was introduced into the above solution and stirred vigorously for 10 minutes. Then the sediment was centrifuged, washed repeatedly with ultrapure water, and finally vacuum dried at 60°C .

Syntheses of PdCu Ngs

Firstly, 14.4 mg of Cu₂O nanocages powder was dispersed in 20 ml of ultrapure water. Then, 135 mg PVP was added, ultrasonic treatment was performed for 5 min, and then stirred for 3 min, 10ml H₂PdCl₄ (10 mM) aqueous solution was added to the above mixture and continuously stirred for 20 min. Subsequently, 40 μL CH₃COOH was injected and the reaction continued for 40 min to remove the Cu₂O template. The obtained precipitate is collected by centrifugation, washed with a mixture of ultrapure water and ethanol, and then dried under vacuum at 40°C for 5 h. We prepared (PdCu Ngs 2) and (PdCu Ngs 10) by adjusting the dosage of H₂PdCl₄ (2ml,10ml).

Syntheses of PdCuB Ngs

For a typical synthesis of PdCuB nanocages, a certain number of pre-synthesized PdCu nanocages are dispersed in 10 mL DMF. 2 mL NaBH₄ (25 mg/mL) was added to the above dispersion and stirred in an ice water bath for 2h. The product was collected by centrifugation and washed with ethanol and ultrapure water. Finally, PdCuB Ngs were obtained by vacuum drying at 40°C for 5h.

Electrochemical Measurements

The electrochemical performance of the catalyst was tested on CHI660B electrochemical analyzer produced by Shanghai Chenhua Instrument Co. Ltd. The electrochemical tests were carried out in a standard three-electrode system at 25°C, which comprises a glassy carbon electrode with a diameter of 4mm coated with catalyst as the working electrode, a Pt sheet with an area of 1cm² as auxiliary electrode, and an Hg/Hg₂SO₄ electrode as reference electrode. All potentials mentioned in this study were referenced to the Hg/Hg₂SO₄ electrode. All solutions were prepared using ultrapure water from Millipore, which has a resistivity of 18.2 MΩ cm. To prepare the working electrode, we dispersed 0.8 mg catalyst and 3.2 mg Vulcan XC-72 carbon by ultrasonic oscillation in 2 ml solution containing ethanol and 5 wt% Nafion to obtain a suspension. After that, we applied 10 μL catalyst suspension onto the surface of the glassy carbon electrode and left it to dry in the air. Finally, 5 μL 5 wt% Nafion was dropped on the obtained electrode.

Cyclic voltammetry (CV) tests were performed in a 0.5 mol L⁻¹ H₂SO₄ solution or a 0.5 mol L⁻¹ H₂SO₄ solution that contained 0.5 mol L⁻¹ HCOOH, with a potential range of -

0.63 V to 0.32 V at a scanning speed of 50 mV/s. Electrochemical impedance spectra (EIS) were obtained at 100 kHz and 0.01 Hz using a solution of 0.5 mol L⁻¹ H₂SO₄ and 0.5 mol L⁻¹ HCOOH at -0.45 V. To acquire the amperometric I-t curves, a solution of 0.5 mol L⁻¹ H₂SO₄ and 0.5 mol L⁻¹ HCOOH was used at -0.4 V. Before any electrochemical tests were conducted, the electrolyte was deprived of oxygen using high-purity nitrogen.

Electrochemical active surface area (ECSA) presented in this work is calculated according to the PdO reduction peak in CV curve. The specific formula is: ECSA = $Q_{PdO}/(420 * m_{Pd})^1$. In the given equation, Q_{PdO} (μC) represents the charge absorbed by oxygen during the process of underpotential deposition. The charge density for oxygen adsorbed on a monolayer of Pd is 420 $\mu C cm^{-2}$, while m_{Pd} denotes the mass of Pd loaded onto the glassy carbon working electrode.

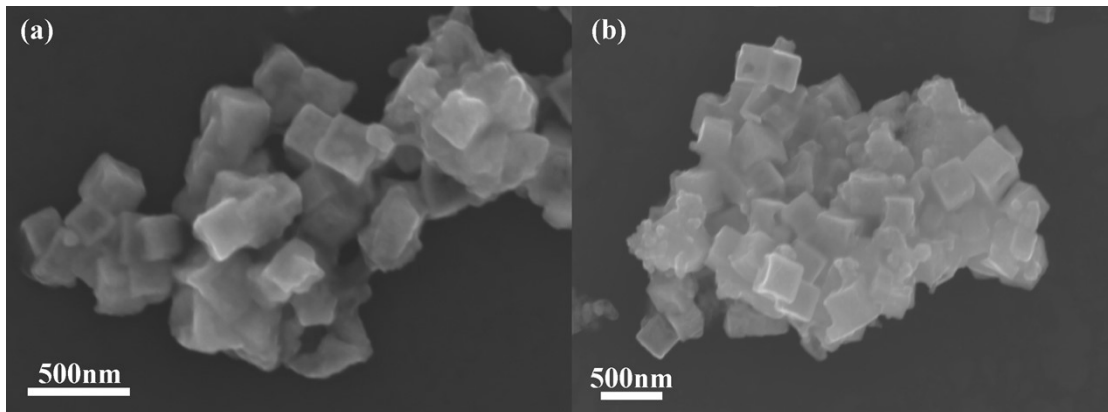


Fig. S2 The SEM images of (a) (PdCu Ngs 2) and (b) (PdCu Ngs 10)

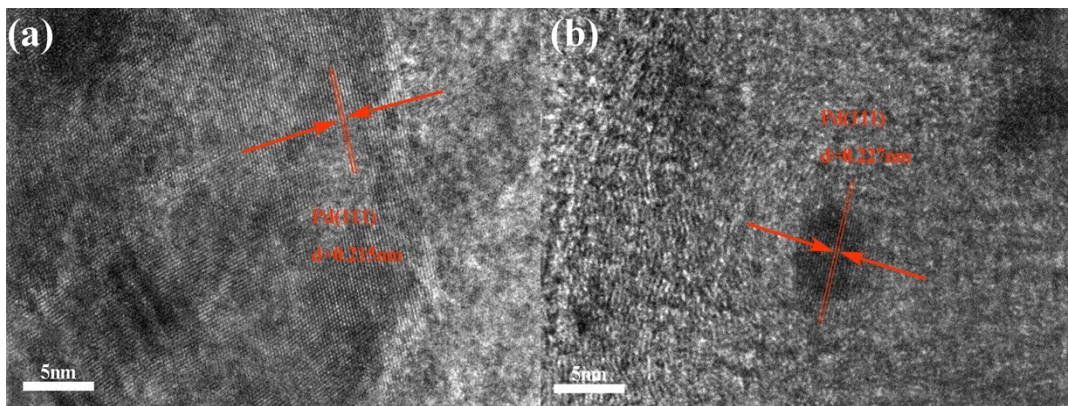


Fig. S3 The HRTEM of (a) PdCu Ngs, (b) Pd/C.

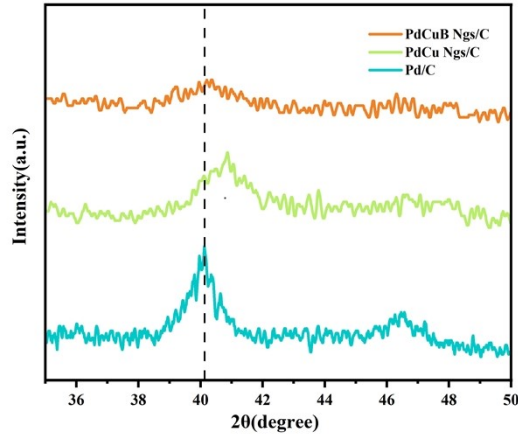


Fig. S4 XRD amplified parts between 35°~ 50°.

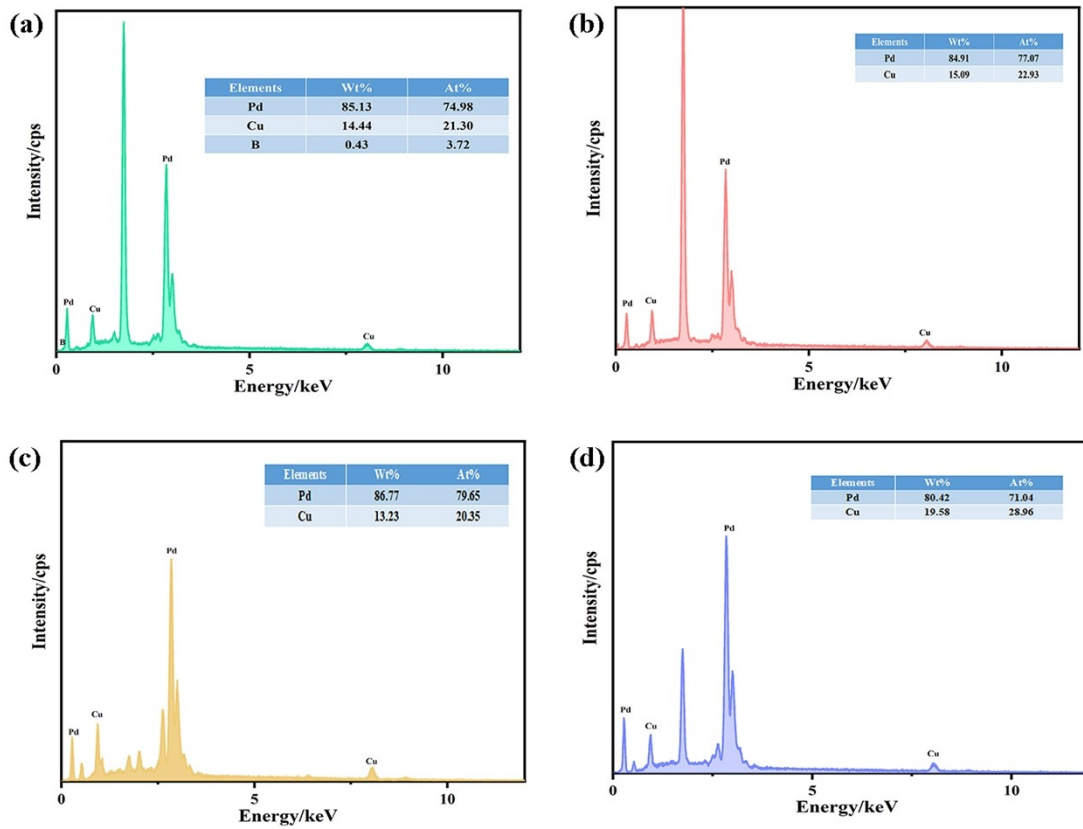


Fig. S5 The EDX of (a) PdCuB Ngs, (b) PdCu Ngs 6, (c) PdCu Ngs 10 and (d) PdCu Ngs2.

Table S1 The results of Pd3d peaks fitting in the XPS spectra of Pd/C, PdCu Ngs/C, and PdCuB Ngs/C catalysts.

Catalyst	Binding energy (eV)	species	Relative ratio (%)
----------	---------------------	---------	--------------------

Pd/C	336.0	Pd metal	46.20
	337.9	Pd (II)	20.46
	341.2	Pd metal	23.10
	343.2	Pd (II)	10.24
PdCu Ngs/C	335.9	Pd metal	46.64
	337.8	Pd (II)	20.03
	341.1	Pd metal	23.32
	343.1	Pd (II)	10.01
PdCuB Ngs/C	336.0	Pd metal	53.01
	337.9	Pd (II)	13.65
	341.2	Pd metal	26.51
	343.2	Pd (II)	6.83

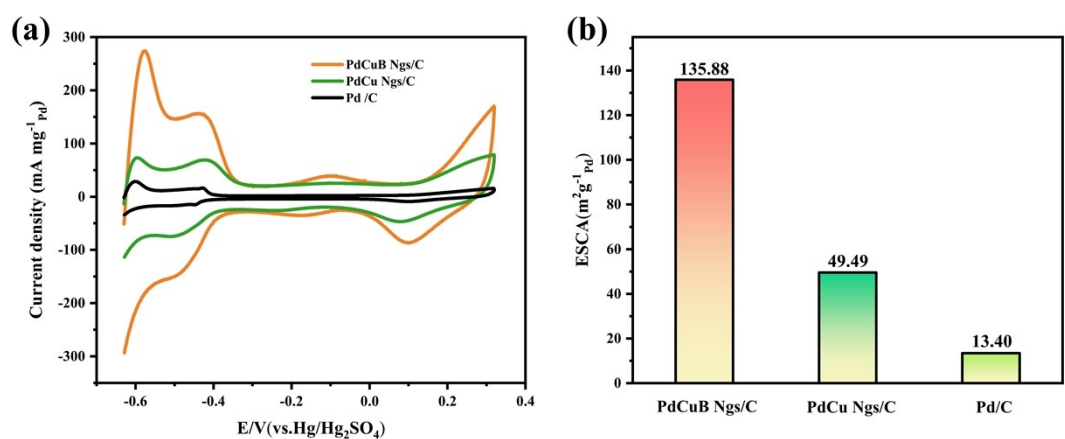


Fig. S6 (a) CV curves of the PdCuB Ngs/C, PdCu Ngs/C, and Pd/C catalysts in N₂-saturated 0.5 mol L⁻¹ H₂SO₄ solution and (b) corresponding ECSAs

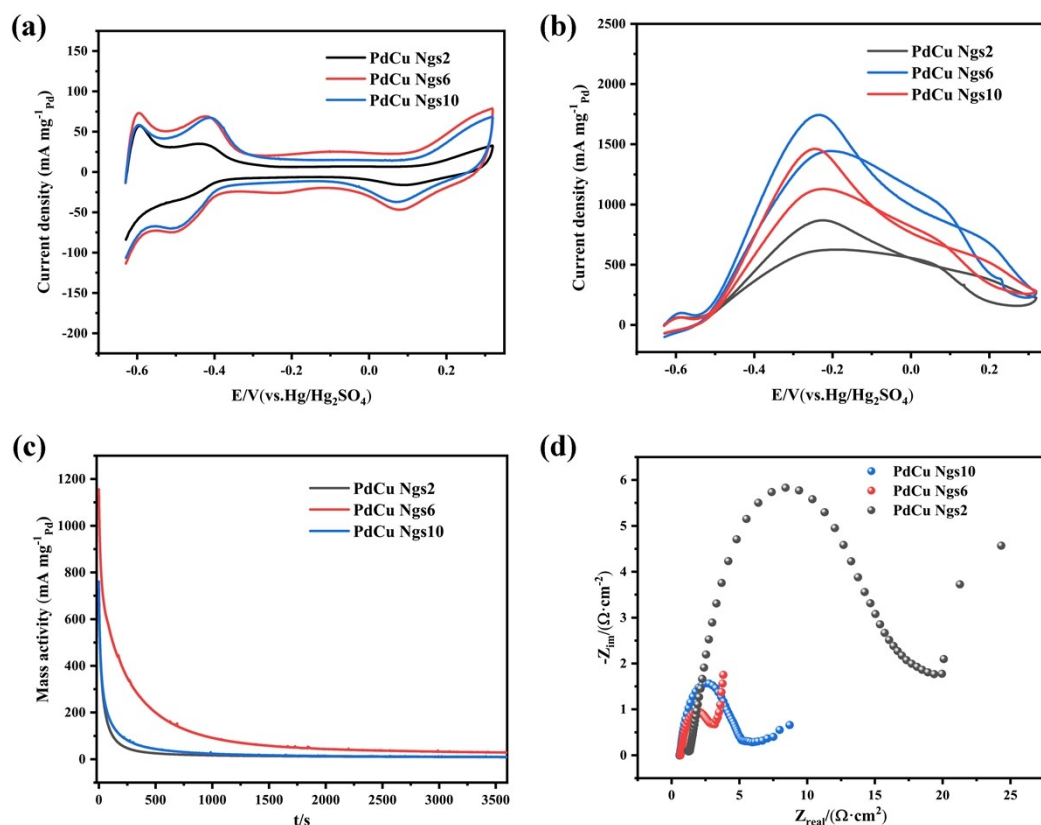


Fig. S7 The Electrochemical characterization of PdCu Ngs 2, PdCu Ngs 6 and PdCu Ngs10 catalysts (a) CV curves in N_2 -saturated $0.5 \text{ mol L}^{-1} \text{ H}_2\text{SO}_4$ solution, (b) CV curves of in N_2 -saturated $0.5 \text{ mol L}^{-1} \text{ H}_2\text{SO}_4 + 0.5 \text{ mol L}^{-1} \text{ HCOOH}$ solutions, (c) Amperometric $i-t$ curves at -0.4 V in N_2 -saturated $0.5 \text{ mol L}^{-1} \text{ H}_2\text{SO}_4 + 0.5 \text{ mol L}^{-1} \text{ HCOOH}$ solution, (d) EIS experiments.

The strongest XRD diffraction peak in the PdCu Ngs catalyst is located between the (111) plane of Pd(40.11°) and Cu(43.30°), confirming that the PdCu structure of the alloy has been formed. XPS results show that the Pd 3d peak of PdCu Ngs catalyst has a negative shift relative to Pd/C catalyst to a certain extent, indicating that there is an electronic effect between Pd and Cu, which regulates the electronic structure of Pd, thereby improving the activity and stability of the catalyst. The enhanced catalytic activity of PdCu Ngs can be attributed to the optimized electronic structure and the generation of more accessible active sites due to the synergistic effect of Pd and Cu. We further performed electrochemical tests on different proportions of PdCu Ngs to explore the optimal proportions. Stable cyclic voltammety curves of PdCu Ngs2/C,

PdCu Ngs6/C and PdCu Ngs10/C catalysts in N_2 saturated $0.5 \text{ mol L}^{-1} H_2SO_4$ solution. According to the formula, ECSA of PdCu Ngs 2/C and PdCu Ngs 10/C are 49.39 and $38.59 \text{ m}^2 \text{ g}^{-1}_{Pd}$, respectively, which are both smaller than PdCu Ngs/C (namely PdCu Ngs6/C). As shown in Fig. S7b, the peak current density of PdCu Ngs2/C and PdCu Ngs10/C for formic acid oxidation are 868.29 and $1567.83 \text{ mA mg}^{-1}_{Pd}$, respectively, which are smaller than that of PdCu Ngs/C. It can be found from the amperometric *i-t* curves that the current density of PdCu Ngs/C at 3600s is higher than that of the other two catalysts, indicating that PdCu Ngs/C has the best stability. EIS test shows that PdCu Ngs/C has the fastest formic acid oxidation kinetics. In summary, PdCu Ngs/C catalyst has the best electrocatalytic activity and stability for formic acid oxidation among the three samples. The above results indicate that too low Cu content in the catalyst can not achieve the best synergistic effect of Pd and Cu, while too high Cu content weakens the performance of Pd as the main catalyst. Therefore, in the subsequent synthesis of PdCuB Ngs catalyst, we doped B based on this catalyst.

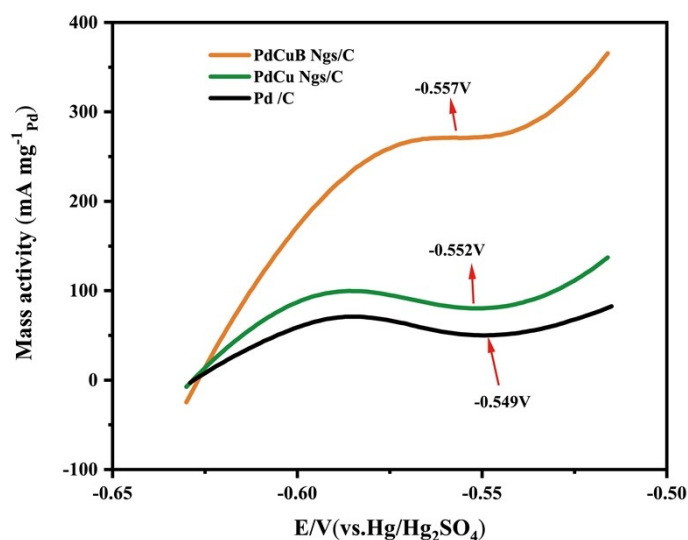


Fig. S8 CV amplified parts before -0.52V

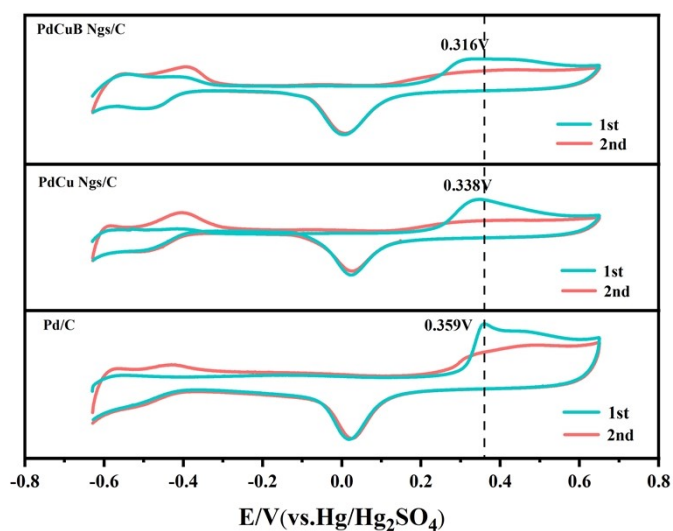


Fig. S9 CO stripping voltammograms of the PdCuB Ngs/C, PdCu Ngs/C, and Pd/C catalysts in CO-saturated 0.5 mol L⁻¹ H₂SO₄ solution.

Based on the above experimental results, we speculated that PdCuB Ngs/C catalyst can kinetically accelerate the removal of toxic intermediate CO. Therefore, the effect of removing CO by catalyst was directly detected by electrochemical CO anti-poisoning experiment. Fig. S9 illustrates CO stripping voltammograms of three samples. In the first cycle, the observed oxidation peak within the potential range of 0.30 to 0.37V corresponds to the oxidation peak of CO adsorbed on the catalyst surface. In the second cycle, the hydrogen adsorption areas reappear and the CO oxidation peak disappears. This result shows that the monolayer adsorption of CO intermediates on the catalyst surface is almost completely oxidized. Meanwhile, it can also be found in Fig. S9 that the peak potentials of CO oxidation on PdCuB Ngs/C, PdCu Ngs/C and Pd/C are 0.316, 0.338 and 0.359V, sequentially. The oxidation peak potential of CO on PdCuB Ngs/C catalyst shifts negatively by 21 and 43 mV compared with PdCu Ngs/C and Pd/C, respectively. Obviously, both the initial oxidation potential and the peak potential of CO have significant negative shifts on PdCuB Ngs/C, which corresponds to easier CO oxidation, indicating that PdCuB Ngs/C possess exceptional resistance to CO poisoning. This suggests that the introduction of Cu and B greatly weakens the adsorption strength of CO on the Pd surface. Since the removal of the adsorbed CO toxic intermediates plays a decisive role in electrocatalytic FAOR, it is further verified

that ternary alloy PdCuB Ngs has a kinetical enhancement effect on electrocatalytic FAOR. Therefore, the PdCuB Ngs/C obtained exhibits high electrocatalytic activity and excellent durability, and is an ideal candidate material for efficient electrocatalysts in practical DFAFC systems.

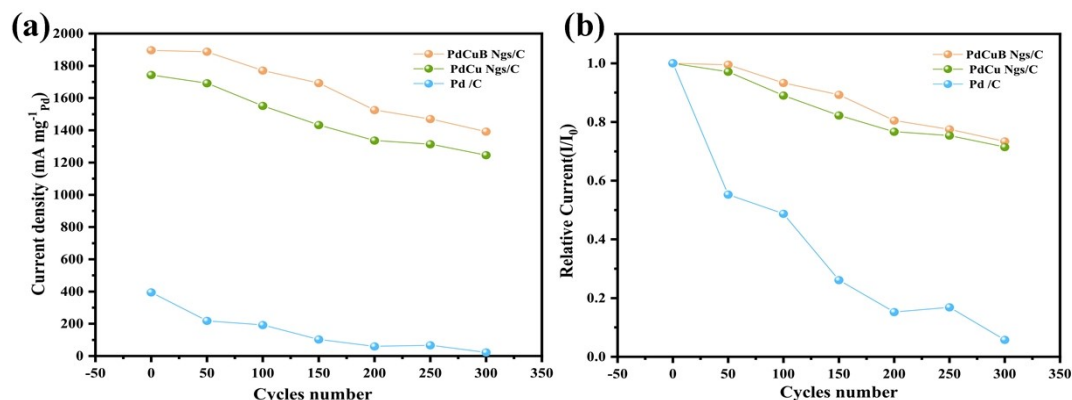


Fig. S10 (a) Stability test; (b) the normalized peak current plots for PdCuB Ngs/C, PdCu Ngs/C and Pd/C.

To further demonstrate the durability of the PdCuB Ngs/ C catalyst, CV was performed for long-term operation in N₂-saturated 0.5 mol L⁻¹ H₂SO₄ and 0.5 mol L⁻¹ HCOOH solutions. The curves of peak current density of three samples with the number of cycles are provided in Fig. S10a. Obviously, the prepared PdCuB Ngs/ C catalysts exhibit better electrochemical stability than Pd/C, PdCu Ngs/C. In Fig. S10b the peak current density of PdCuB Ngs/ C remained at about 73.40% after 300 cycles, which was much better than that of Pd/C (only 5.81%), and slightly higher than PdCu Ngs/C (71.48%).

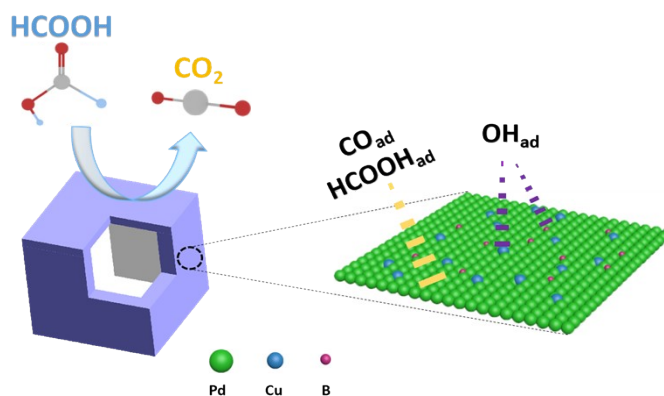


Fig. S11 Schematic illustration of the enhanced electrocatalytic performance mechanisms of PdCuB Ngs catalyst.

Notes and references

1. X. Tai, B. Wu, J. Bao, W. Qu, L. Zhao and Z. Wang, *Materials Today Sustainability*, 2022, **18**.